

This is an Accepted Manuscript of an article published by Taylor & Francis in International Journal of Geotechnical Engineering on 03/03/17, available online:  
<http://www.tandfonline.com/doi/abs/10.1080/19386362.2017.1297552>

## **Abstract**

Three dimensional finite element analyses were carried out to study the geotechnical behaviour of piles fitted with high-density polyethylene (HDPE) tubes as energy loops for harnessing ground heat. The objective was to examine whether the existing analysis methods for conventional piles are applicable to energy piles. Using *PLAXIS 3D* software, simulations were done for 60 cases of energy piles comprising variously configured HDPE tubes. It was found that HDPE tubes inevitably interact with the soil around the pile such that 6-11 HDPE tubes decreased the load capacity by 18%-70%, while 3-4 HDPE tubes had an optimum reinforcing effect on the soil, thereby increasing the load capacity by 30%-75%, depending on the pile size. However, the tubes had little effect on settlement at ultimate load. Thus the work highlighted the limitation of conventional methods of analysis and the geotechnical effect of HDPE tubes installed to protrude from the base of an energy pile.

**Key words:** *Energy piles, Capacity, Settlement, Sand, Finite element analysis*

## **Introduction**

With the present emphasis of sustainability in development, there is an ever increasing need to find energy resources alternative fossil fuels, minimise carbon emissions, reduce waste and promote recycling / re-use of materials. Geothermal energy or ground source heat pump has been used for internal heating and heating of bathing water since the ancient Roman times. Geothermal energy can be collected by trench collectors, flat collectors, or borehole heat exchangers up to a depth of 300 meters. These systems have been used for many years in different countries, most notably Austria, and presently the number of installed heat pumps is in excess of a hundred thousand. Suryatriyastuti et al. (2012) and Happold (2013) identified two kinds of ground heat exchangers: (a) open-loop and (b) closed-loop system. In an open-loop system, water from an aquifer is extracted by a heat pump into a building for heating purposes. In a closed-loop system (also referred to as a borehole heat exchanger), geothermal energy is transferred from the ground to a heat pump by absorber pipes that are laid either horizontally such as energy cages and horizontal collectors or vertically such as boreholes and energy piles. Currently there is no authoritative geotechnical design manual such as a Eurocode for energy piles and engineers mainly rely on specialist literature available in Skanska (2012, 2013), Abdelaziz et al. (2011) and others.

Constructing energy piles involves incorporating heat exchangers inside piles or diaphragm walls such as shown in **Fig. 1**.



**Figure 1: Reinforcement cage and energy tubes installed in a large diameter, bored cast in-situ pile (Skanska, 2013).**

At present limited information is available regarding the likely effects of energy loops on the load carrying capacity and settlement behaviour of energy piles, yet clearly there will be some degree of interaction between the loops and the pile-soil system. This is because the loops protrude in bundles from the pile into the highly stressed soil zone beneath the pile base under base resistance mobilised. In an attempt to address the current deficiency in knowledge, some researchers notably Ozudogru et al. (2014) have attempted to develop *3D* numerical models but with limited success in or focus on how energy piles may mobilise resistance differently to conventional piles. A successful numerical analysis and evaluation of the influential parameters for energy piles would immediately provide engineers with a new methodology for analysing such piles. It is hoped that as the use of energy piles become more commonplace, case records of full-scale pile testing will avail new data that could be used to validate the numerical results reported in this paper.

## **Some case studies of load tests and analysis of energy piles**

First trialled in the UK by Skanska (2010a, 2010b), the technology behind energy piles is still developing and is the focus of dissemination by several publications e.g. Skanska (2012, 2013), Bouazza (2011), Ozudogru et al. (2014), Laloui and Didonna (2011) and Abdelaziz et al. (2011), among others. Some case histories of energy pile testing and analysis are presented and reviewed below.

### *(1) Energy pile test at Lambeth College, London (Bourne-Webb et al. 2009)*

This case record emanated from the design and construction of a 5-storey building for Lambeth College in South London, UK. The building foundation system was to comprise 143 bored cast in-situ piles of 0.6 m diameter by 19 m to 24 m lengths and fitted with pipe loops as part of a ground-source heat pump system. The piles, which were installed in London clay, had working loads in the range 1025 kN to 1350 kN. To aid the design of the contract piles, two of the piles were planned to be tested with applied loads up to 1.5 times the working load, although further tests were conducted on one of the piles (a sacrificial pile) by applying thermal cycles and a maintained load of up to 3600 kN. This was to study the resulting effects on axial force distribution and load-settlement behaviour of the energy piles.

The upper 5 m segment of the test pile shaft was sleeved through the superficial layer of Made Ground and River Terrace Deposits. The strain gauge readings in this upper isolated segment not in contact with the soil were used to derive the pile stiffness as built. The pile was cast with six 32mm diameter longitudinal bars and hoop reinforcement. The test pile was fitted with 4 HDPE tubes and a range of instruments including vibrating wire strain gauges embedded at 6 levels along pile (3 gauges symmetrically disposed at a cross-section), 6 thermistors, optical fibre sensors, linear variable displacement transducers and load cells. A 4 MN pile test rig jacking against 4 anchor corner piles was used to load test the energy pile, which lay at the centre of the test frame. A large shipping container housing an 8 kW heat pump and optical fibre sensor data logger was placed on ground in between the pile test rig and a heat sink pile that connected the supply and return tubes to the heat pump to produce the desired thermal cycles to the test pile. An instrumented borehole was sunk 0.5 m from the test pile to enable profiling of temperatures that closely represented the field conditions.

The heat sink was also provided with optic fibre connection to the data logger housed in the container. Another data logger provided in the heat pump allowed monitoring of the fluid outflow

and return temperatures for both the test pile and the heat sink pile. Thermal test cycles were selected to give an extreme case of temperature range  $-60^{\circ}\text{C}$  to  $+56^{\circ}\text{C}$  (over period of 1-2 weeks), with the heat pump operating at its maximum output. Obviously this range of temperature is purely for academic study as it is beyond the typical of heating/cooling of  $-1^{\circ}\text{C}$  to  $+30^{\circ}\text{C}$  (over period of hours or days) for actual energy piles in practice. From the pile test results and mechanisms inferred, it was revealed that:

- (a) the coefficient of thermal expansion for the pile was approximately  $8.5 \times 10^{-6} \text{ m/m}^{\circ}\text{C}$ , which is consistent with typical values reported for limestone aggregate-based concrete
- (b) the cooling and heating cycles induce pile axial forces (which can be additive or subtractive) whose magnitudes and senses depend on the restraint conditions at the pile ends.
- (c) under applied pile head loading alone the pile is obviously in compression and the pile shaft shear stresses act upward (resists pile loading)
- (d) under cooling of a pile unrestrained at both ends, the pile contracts so any restraint applied to the pile leads to positive and negative skin friction along the upper and lower parts of the pile respectively
- (e) under heating the pile extends and any restraint applied to the pile shaft leads to negative and positive skin friction along the upper and lower segments respectively
- (f) as a consequence of the mechanisms in (c) and (d) above, it is possible for the additional pile concrete stresses to exceed the values designed for if the pile is treated as a conventional pile ignoring the thermal effects. However, there is also a fortunate implication in that there is an increased margin between the pile ultimate shaft resistance and the pile-soil interface shear stresses induced by thermal loading of the pile. In the test, the peak unit shaft resistance mobilised in any thermal cycle was 75 kPa, which was still lower than the value 90 kPa measured in a destructive loading test undertaken on the pile subsequent to the cyclic thermal test. Hence the thermal mechanism becomes unlikely to affect the geotechnical capacity of the energy pile.

(2) *Pile testing at the US Air Force Academy in Colorado Springs (Khosravi et al. (2016))*

Eight energy piles were installed as foundations for a building at a US Air Force Academy in Colorado Springs. One of the working piles was tested as part of a research project aimed at investigating the axial stress and strain response of the piles in thermo-mechanical loading. The soil profile at the site comprised 1 m thick sandy fill overlying 1 m thick dense sand which in turn was underlain by a deep stratum of sandstone into which the pile penetrated by 13.6 m. Various types of instruments were installed in the test pile including vibrating wire strain gauges positioned at 9

levels along the pile, as well as 10 thermistor strings to measure the temperature variations in the soil around the test pile. A series of loops of HDPE heat exchanger tubing of 20 mm nominal diameter were attached inside the pile reinforcement cage and a heating unit installed to impose different cycles of heating and cooling on the pile. Heated water was circulated for 498 hours, after which cooling was effected for 700-1200 hours. During the heating and cooling cycles the pile instrumentation readings were recorded at times corresponding to mean temperature steps  $\Delta T$  of 6°C. The maximum temperature applied was 30°C (heating cycle) representing an overall pile temperature rise of 18°C above the ambient value of about 12°C.

Khosravi et al. (2016) adopted an axi-symmetric finite difference method in FLAC 2D software to simulate the pile behaviour during the heating and cooling cycles. Mohr-Coulomb failure criterion was assumed for the soil and the pile was modelled as a perfectly linearly elastic material. The input properties of the pile and soil were: bulk modulus, shear modulus, thermal conductivity, specific heat extraction, coefficient of thermal expansion and Poisson's ratio. The soil-pile interface input properties were: normal stiffness, shear stiffness, cohesion and friction angle. The tests showed that as the larger the applied pile head load the greater was the thermal axial stress in the upper segment of the pile while there was very little effect on the lower part of the pile, where the main influential factor on was thought to be the stiffness of the soil below the pile base (fixity condition). The maximum thermal axial stress predicted from FLAC 2D was found to be close to the measured value (6.8 MPa compared with 6.45 MPa). It was also inferred that the resistance of the soil surrounding the pile influences the distribution of thermal axial stress and strain in the pile considerably. High soil stiffness led to higher thermal axial stress and lower thermal axial strain.

(3) *Pile test for a building in Hokkaido, Sapporo, Japan (Hamada et al. 2007)*

This case study relates to thermal rather than geotechnical performance of energy piles. Energy piles were installed as part of the foundations for a two-storey reinforced concrete building incorporating a semi-basement and used as an office cum residential property. The building, which had a plinth area of up to 247.53 m<sup>2</sup> was completed in the year 2000. The energy piles, working mainly as friction piles, were to for the purpose of air conditioning with cooling derived from an underground thermal system that was to be powered by a heat pump. Tests were carried out on 3 energy piles to aid the design and specification of the heat exchanger to be fitted inside the piles. Based on energy efficiency and cost of provision, it was decided to use an underground brine-circulating heat exchanger of U-tube type. From the tests, continuous and long term observations

indicated that the seasonal average temperature of the ground-cooled brine returning to the building was 2.4°C whereas the pile surface temperature was 6.7°C on average. With the energy pile system in use, the seasonal average savings in energy was about 23% when compared to conventional air conditioning systems.

*(4) Piling at the Swiss Federal Institute of Technology, Lausanne, Switzerland (Laloui et al. 2006)*

Field thermal tests were carried out on a heat exchanger pile, with comprehensive instrumentation, as part of the foundations for a new building at the site described above. Increasing head loads resulting from each constructed storey were applied to the pile with simultaneous imposition of heating and cooling cycles, during which the axial force distribution in the pile was monitored using fibre optic sensors, extensometers and base load cell. The final storey exerted a load of 1300 kN at which stage an applied thermal cycle of 15°C heating resulted in approximately 100% increase in axial force, with a more marked increase recorded at the pile base level. This typical behaviour of an energy pile is similar to that reported by Bourne-Webb et al. (2009).

Mathematical modelling carried out by Peron and Laloui (2010) further to the pile tests sought to develop a finite element numerical tool for studying the influence of temperature on mechanical behaviour of energy piles. The analyses involved definition of boundary and initial conditions and coupled formulation with displacements, pore pressures and temperatures as the field variables. This led to development of a constitutive model (named ACMEG-T) to account for the change in angle of shearing resistance of soil, thermo-elasticity and thermo-plasticity effects. The model consequently allowed modification to the shaft resistance mobilisation and settlement arising from overall load increase and decrease associated with pile heating and cooling respectively. Numerical simulations indicated the influence of complex non-linear processes relating to the thermo-hydro-mechanical couplings as yet to be properly understood.

### **Comments on the findings from the case studies in the light of the current work**

All the case studies mainly focus on the load-transfer and thermodynamic effects of temperature cycles on an energy pile. In contrast, the present work concentrates on how HDPE loops of different intensities outside and inside a pile body interact with the pile-soil system to influence the carrying capacity and settlement response of an energy pile. Purely for academic study, in most of the pile test cases (for example Bourne-Webb et al. (2009)), the range of applied temperatures and cycle frequencies are extreme and unrepresentative of practical values (typically -1°C to +30 °C of

cooling and heating cycles occurring over periods of hours or days). Furthermore there seems to be consensus that the thermal mechanisms, although important in influencing pile axial stresses, are unlikely to affect the geotechnical capacity of the energy pile. This is primarily due to the beneficial effect of pile head restraint conditions, which for real pile foundations, lead increased margin between the pile ultimate shaft resistance and the pile-soil interface shear stresses induced by the thermal loading (Bourne-Webb et al. (2009)). It is therefore imperative that the emphasis of the present work be on how the intensity and configuration of HDPE loops can impact on pile capacity. As such the parameters of interest here are different to those focussed on by the above case studies. Due to the irregularity and randomness in HDPE loop configuration beneath pile, a 2D analysis such as the axi-symmetric FLAC finite difference method used by Khosravi et al. (2016), would be inapplicable to the analysis of how the concentration of HDPE loops affect pile capacity. Thus the present numerical work calls for a full 3D analysis to cope with the analysis problem.

### **Geotechnical modelling of energy piles in *PLAXIS<sup>TM</sup> 3D***

*Plaxis 3D Foundation* version 1.5 software (PLAXIS, 2006) was used to model stresses and deformations for 60 hypothetical piles fitted with different numbers of energy loops and installed in dry sand. The first was to define the problem geometry with a sand medium, plastic loop structures and a volumetric pile space, which is illustrated **Fig. 2**, as a volumetric unit diameter pile space.

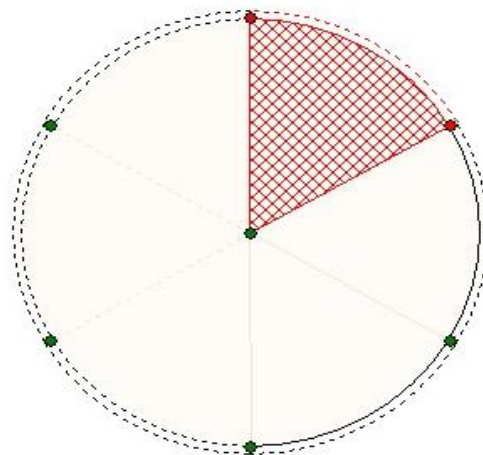


**Figure 2: Volumetric unit diameter pile space in *PLAXIS 3D***

At a later stage, the analysis procedure allows specifying a length to diameter ratio,  $L/D$  of the pile. The marked dots around the pile perimeter are positions (defined in this case by sectors subtending  $60^\circ$  angles) of the energy tubes on the cross-section. The material properties for the pile reinforcement were adopted as linear elastic and non-porous. The sand medium was defined as

unsaturated with a specified unit weight, elastic modulus, poisson ratio and interface reduction factor. The type of finite element used for meshing was 8-noded quadratic tetrahedral elements.

In the present work, a total of 60 energy piles with different  $L/D$  ratios shown in **Table 1** were analysed. These sizes represent a wide range of  $L/D$  ratios from short piles ( $L/D=11$ ) to long slender piles ( $L/D=31$ ) but at the same time the maximum pile length is adopted as 14, in order that the pile base depth values spread from below critical depth to beyond it. This allows the study of bearing capacity (both shaft and base resistance) in variation with pile length. Piling theory teaches that once a critical depth is reached, both the shaft and base capacities no longer increase with increasing depth. For example Braja (2006) quoted a conservative estimate for the critical depth for a pile to be 15 to 20 pile diameters, well near the middle of the range 11-31 used in the current study.

Definition of the geotechnical model of the energy pile needed specifying the contours of the geometry model, setting the units of lengths ( $m$ ) and forces ( $kN$ ), acceleration due to gravity  $g$  and the unit weight of water  $\gamma_w$ . Next, a bore hole was added to the geometry and a soil layer with a top boundary at depth co-ordinate  $z = 0 m$  and bottom boundary at co-ordinates  $z = -14m$  to  $-20m$  depending on the pile length for the case being analysed. This was to allow for the zone of soil shearing beneath the pile by ensuring the pile terminated at least  $6m$  above the bottom limit of the model geometry. The soil around the pile shaft was modelled as a Mohr-Coulomb material and drained. Then the initial stresses in the soil were generated based on  $K_0$  procedure (at-rest lateral earth pressure coefficient). Values of  $K_0 = 0.4122$  were defined for the horizontal effective stresses in both the  $x$  and  $y$  co-ordinate directions of the model space. The properties of the soil were defined as follows: Unsaturated unit weight  $\gamma_{unsat}=17.6 kN/m^3$ ; saturated unit weight  $\gamma_{sat} =20 kN/m^3$ ; Young's modulus  $=19 \times 10^3 kN/m^2$ ; Poisson's constant  $= 0.3$ , reference cohesion  $c_{ref}= 17 kN/m^3$ ; angle of shearing resistance  $\phi=36^\circ$ ; interface reduction factor  $R_{inter} = 1$ .

### **Modelling the energy piles, interface element and HDPE structures**

The energy pile, under downward compression loading from the superstructure, was modelled as a linearly elastic structural column element embedded in the volumetric pile space, with concrete material properties being assigned to the element. Then the element was placed in the sub-soil and interaction with the sub-soil allowed for by introducing a special interface element. The interaction takes into account the load-transfer mechanism and skin friction development, with a distinct relationship between the pile head load and relative pile-soil displacement. To provide the control

scenario, a first analysis case was run for a simple pile not fitted with HDPE loops. This analysis was also used to gauge the relative displacement corresponding to the full mobilisation of the base bearing resistance, for the input soil properties. In *PLAXIS 3D* this control case was created by omitting the pile body from the model and replacing the effect by a point load acting at the ground surface (**Fig. 3**).

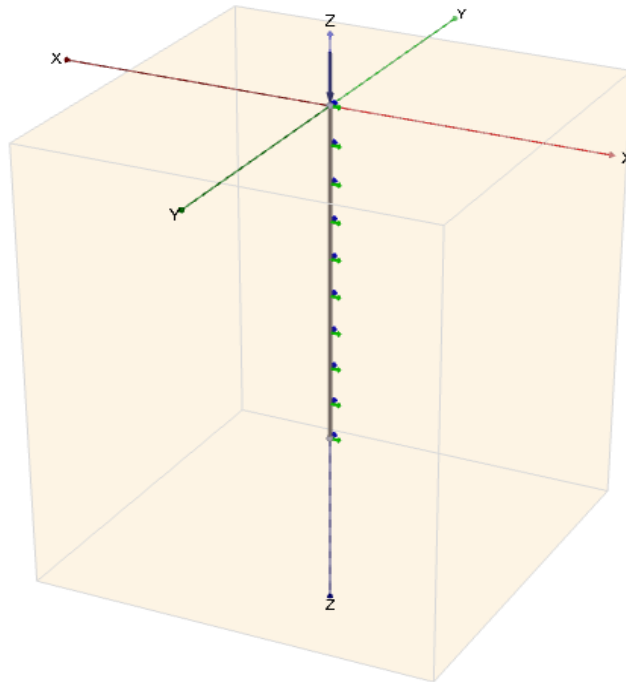


**Figure 3: Representation of loading of simple pile not occupying volume.**

In the analysis of energy piles containing HDPE tubes, the material properties of the tubes had to be defined. The tubes were defined as typically circularly shaped with diameters of 25mm, thicknesses of 3 mm, Young's modulus of  $2.3 \times 10^6 \text{ kN/m}^2$ , unit weight  $\gamma = 8.5 \text{ kN/m}^3$  which of course ought to be less than  $\gamma_w$ . These HDPE properties were used for all pile cases analysed. A finite element mesh for the the problem geometry was generated, with refined regions to take into account the soil stratigraphy as well as the structural objects, loads and boundary conditons. To create a model energy pile in *PLAXIS 3D*, the HDPE tube structures had to be defined and embedded in the simple pile geometry. Although an embedded simple pile was initially regarded as not occupying volume, a particular zone in which plastic soil behaviour is excluded needed to be defined around the pile. This zone represented the elastic zone, the size of which was determined by the pile diameter, to ensure the modelled pile behaved as a volume pile interacting with the HDPE tubes and soil.

In the geometry model, it was not possible to place the HDPE tubes inside the pile because the embedded pile was not recognised as a volume pile by PLAXIS and could not be defined as a hollow pile. Therefore it was necessary to introduce an interface element as shown in **Fig. 4**.

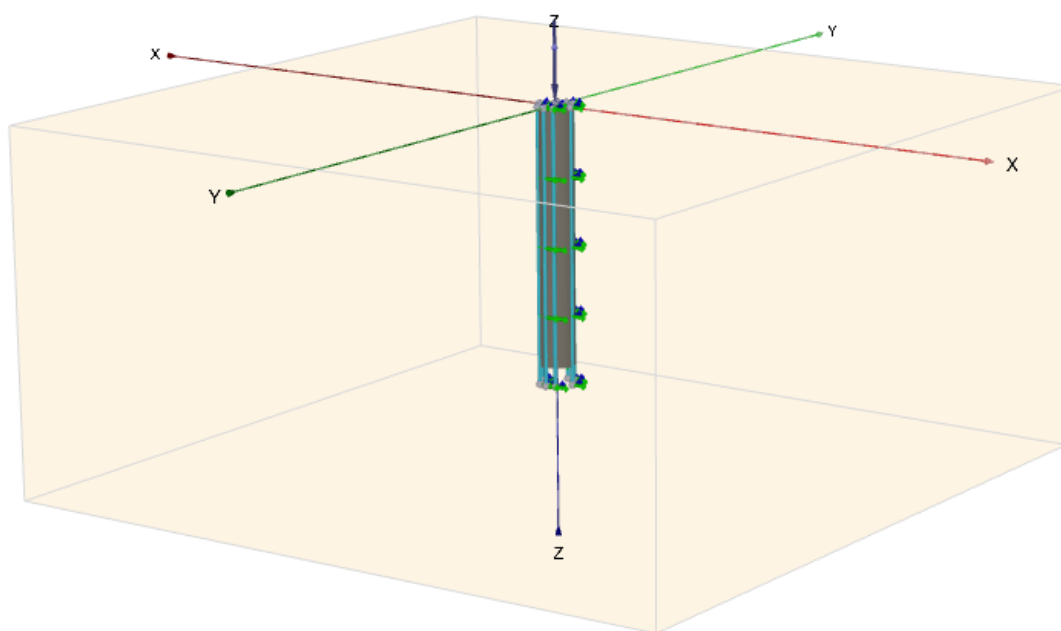


**Figure 4: HDPE tubes attached to the pile interface element and point load acting at pile top**

The interface element itself is pile-shaped and the surface between it and the tubes is defined with the same diameter as the actual pile and having the same material properties as the adjacent soil. This thus allows modelling of the interaction between the pile shaft HDPE tubes with the actual pile body as well as the surrounding soil. So what is seen as the outside surface of the “pile” in **Fig. 4** is actually an interface element interacting with the embedded HDPE tubes.

**Figures 5(a)-(b)** shows an example arrangement of 12 uniformly spaced HDPE tubes attached to the loaded pile, which interacts with the soil.



**Figure 5(a): Modelled HDPE tube structures and external pile loading position**

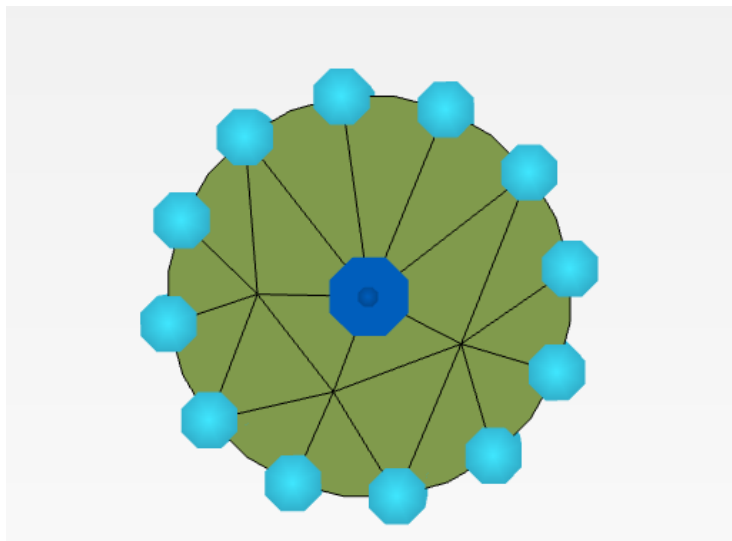


**Figure 5(b): *x-y* plane of pile mesh with interacting HDPE tube structures**

Obviously it was important to ensure that the HDPE pipes extended beyond the pile base into the soil since they connect to heat exchangers in real energy piles. To model the energy loops, a plastic pipe structures was defined with a wall thickness of 3 mm and diameter of 25 mm. Wijewickreme (2011) reported that the HDPE tubes by nature may exhibit time-dependent non-linear response, a

challenge also recognised in the present work to have a potential impact on the accuracy analysis. Additional uncertainties may arise from the usual limitations of applying finite element analysis to complex cases of soil-foundation interaction.

### **Creating and refining the FE mesh for soil layers**

**Figure 6(a)-(b)** depict the FE mesh for a typical soil medium in the model to consist of nearly 23000 elements in most cases analysed.

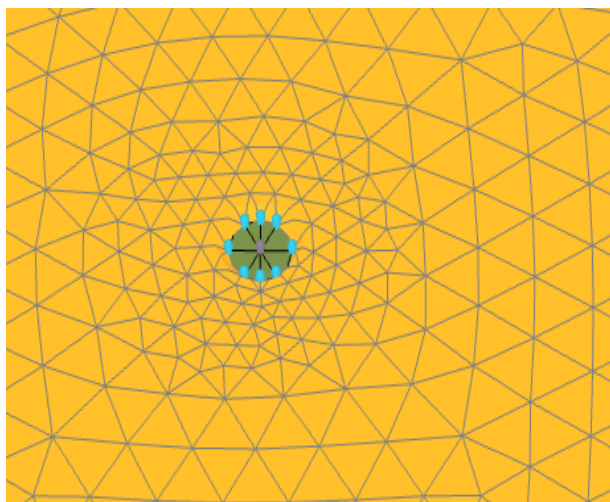


**Figure 6(a): *x-y* mesh plane of soil with pile and HDPE tube structures**

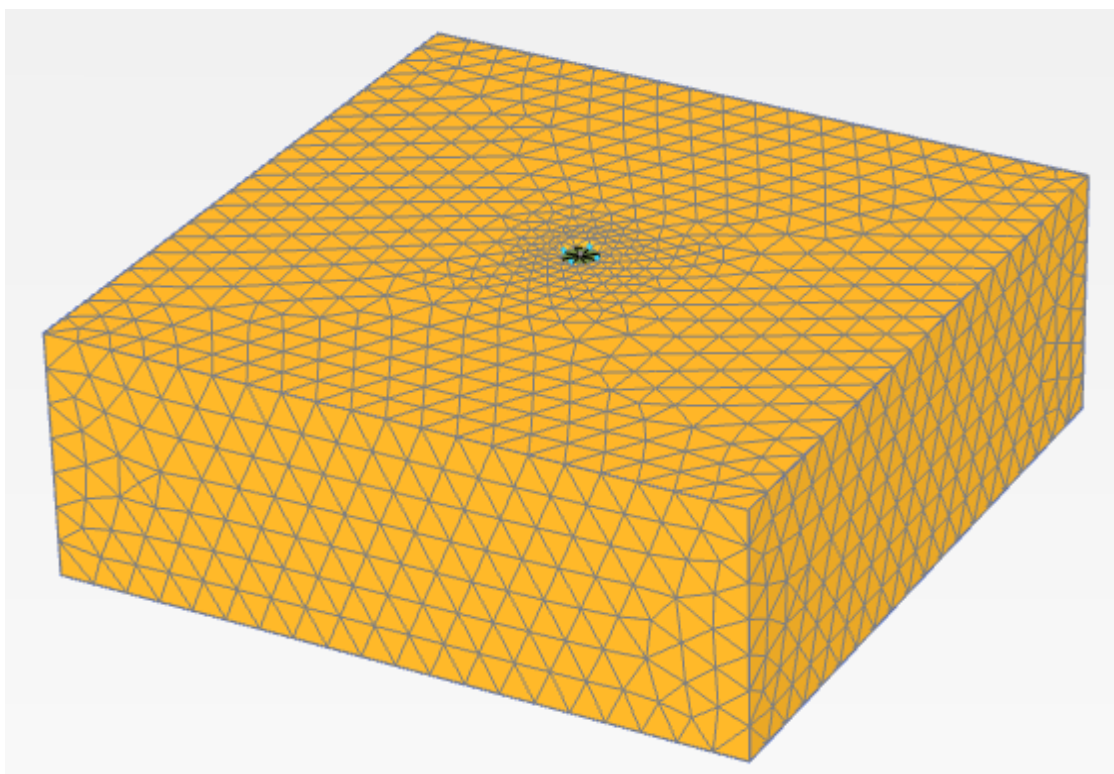


**Figure 6(b): *3D* mesh for soil-pile system and HDPE tube structures**

The elements in close proximity to the pile surface become closer and smaller to increase the accuracy of the computations for the regions of intensive interaction near the structural elements i.e. pile and the HDPE tubes. In order to be compatible with the 8-noded quadrilateral side of a soil element, 16-noded interface elements comprising 8 pairs of nodes were introduced. Along degenerated soil elements, interface elements composed of 6 pairs of nodes were defined so that they were compatible with the triangular sides of the degenerated soil element.

### **Material properties for Soil and interfaces (Mohr-Coulomb model)**

The input values of soil materials and interfaces used for all the analysis cases are given in **Table 2**. Pore pressures were not considered in the analysis due to the high permeability of the sand and low rate of loading as is normal in civil engineering applications.

### **Material properties for piles**

The input values of typical properties for a pile and HDPE tube are given in **Table 3**.

Based upon recent research, Amis (2011) stated that geothermal energy loops should be placed on the outside face of cages where possible. Following this suggestion, the HDPE loops in the PLAXIS pile models were extended away from the pile base by 1 metre as an L-shaped bend into soil as shown in **Fig. 7**.

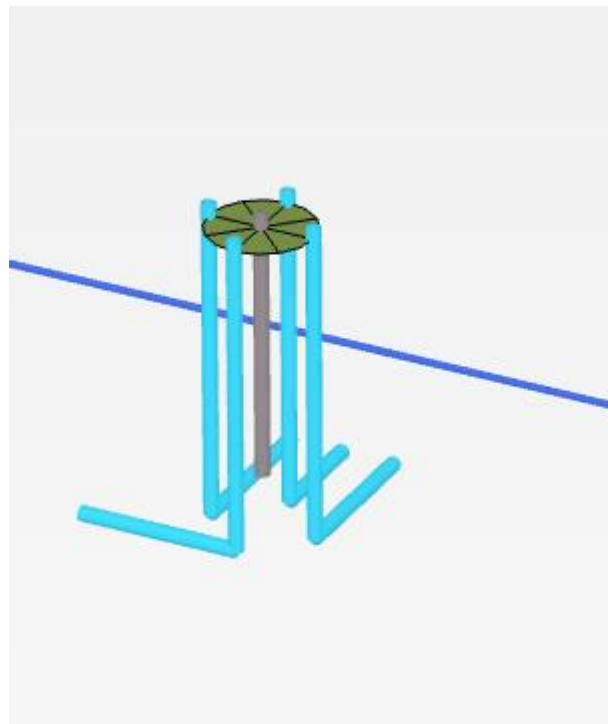


**Figure 7: HDPE tubes modelled to extend into the soil below pile base**

## Results from simulations of the 60 cases of energy piles

Figures 8-11 are colour scheme outputs of computed values of total nodal displacements for cases of different numbers of HDPE tubes fitted in a  $0.45D$  pile model.

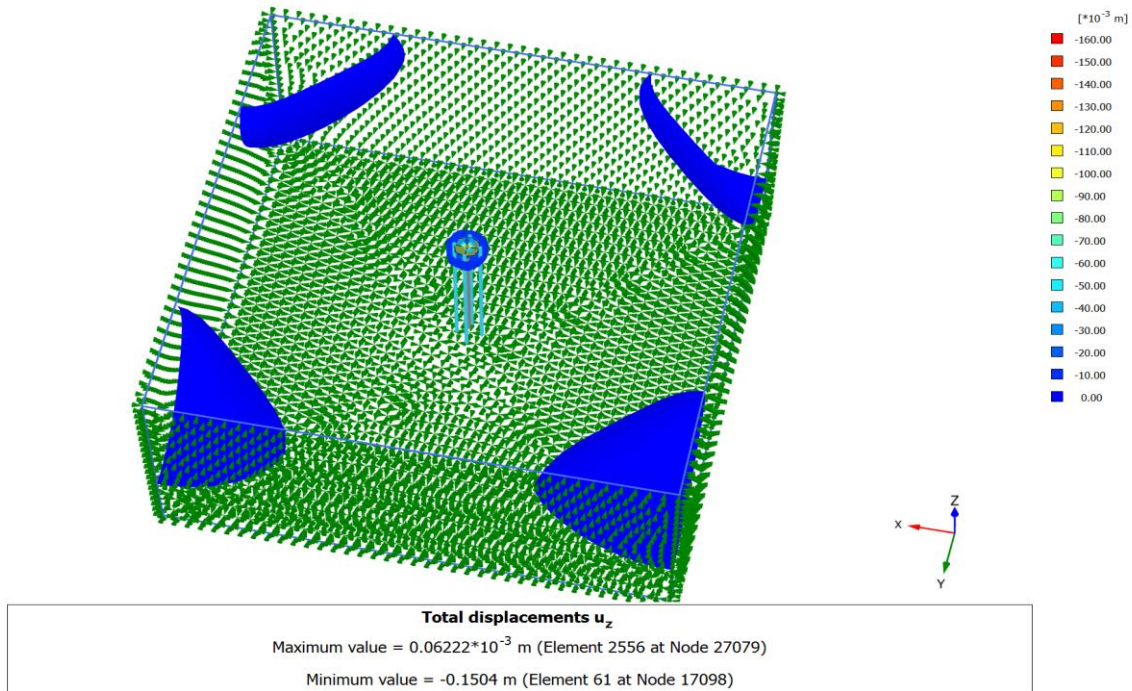
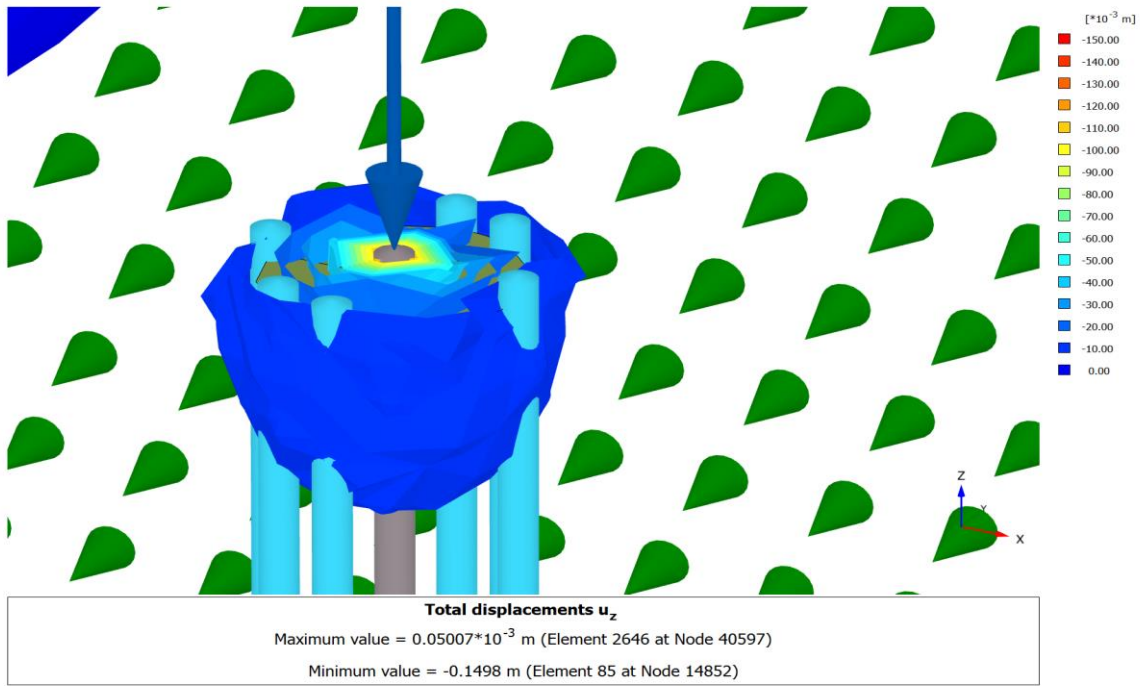
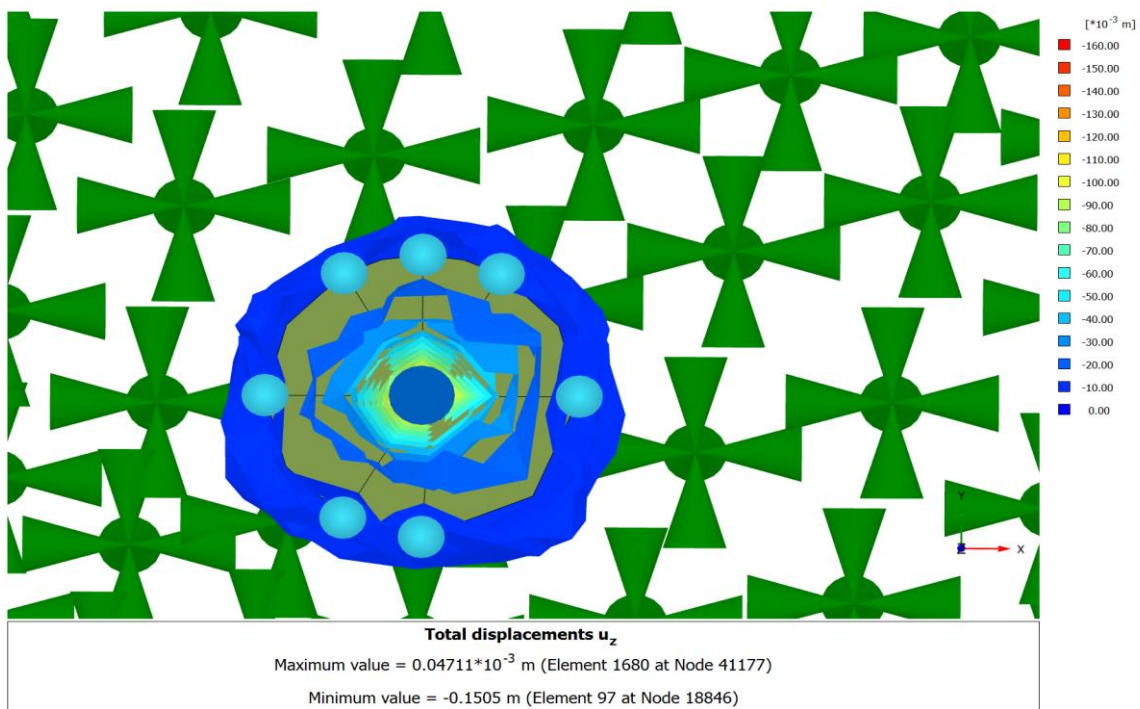


Figure 8: Total displacements from loading of  $0.45D$  pile with 4 HDPE tubes



**Figure 9: Total displacements from loading of 0.45D pile with 6 HDPE tubes**



**Figure 10: Total displacements from loading of 0.45D pile with 7 HDPE tubes**

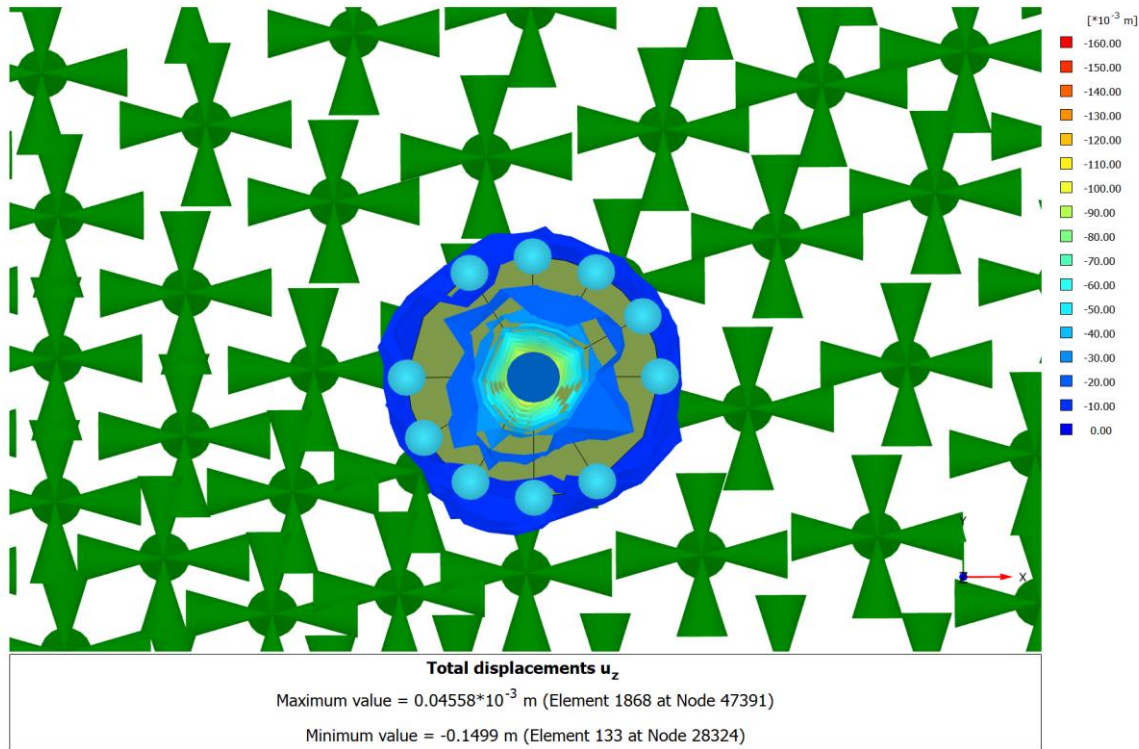


**Figure 11: Total displacements from loading of 0.45D pile with 10 HDPE tubes**

**Tables 4-9** are summarised outputs from *PLAXIS 3D* for the 60 piles analysed. The results are the computed pile capacities and corresponding pile head settlement, for different numbers of HDPE tubes fitted. It is worth noting that the maximum settlements are consistent with piling theory in that they equate to approximately 10 times the pile diameter. This gives some confidence that the models and parameter values used in *PLAXIS 3D* are reliable. Furthermore, the assessed load capacities for the conventional pile cases (i.e. without HDPE tubes) are consistent with estimates from refined soil mechanics formulae (e.g. Fleming et al, 2008) that take into account the effect of high confining stress at maximum pile resistance on the operational value of the: (i) angle of shearing resistance (hence the  $N_q$  bearing capacity factor) and (ii) the density index of the sand in the immediate vicinity of the pile base.

From the *PLAXIS 3D* analyses, the computed pile head capacities are plotted against number of HDPE tubes, for the 6 piles having different  $L/D$  ratios, as illustrated in **Figs. 12-17**. These reveal that the presence of 11 HDPE tubes decreases the pile capacity by up to 70%. However, 3-4 HDPE tubes tend to have an optimal reinforcing effect on the soil around the pile base, hence leading to a 30%-75% increase in pile capacity. These findings seem sensible from a numerical modelling

viewpoint but will need further validation when full-scale test data from energy piles become available in the future.

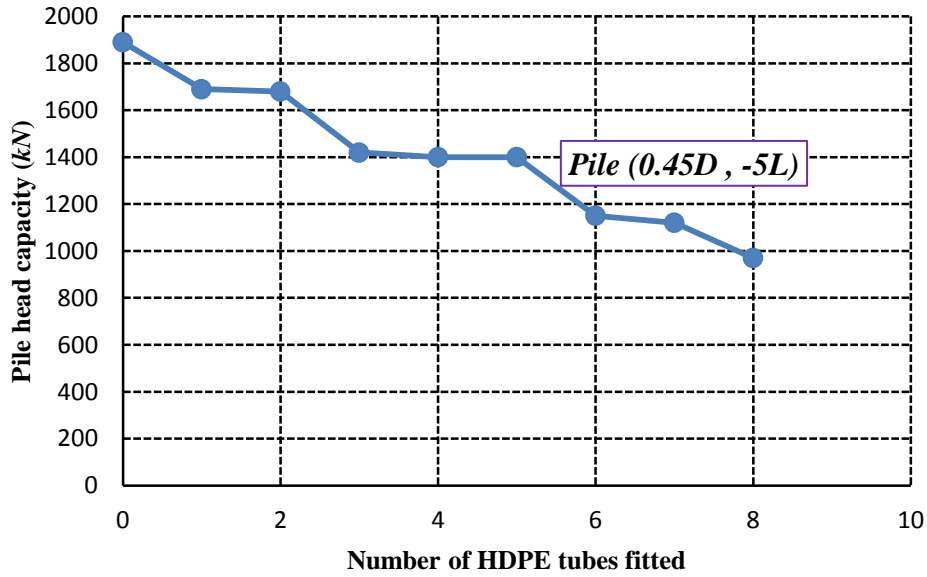


Figure 12: Pile capacity versus number of HDPE tubes for pile (0.45D, -5L).

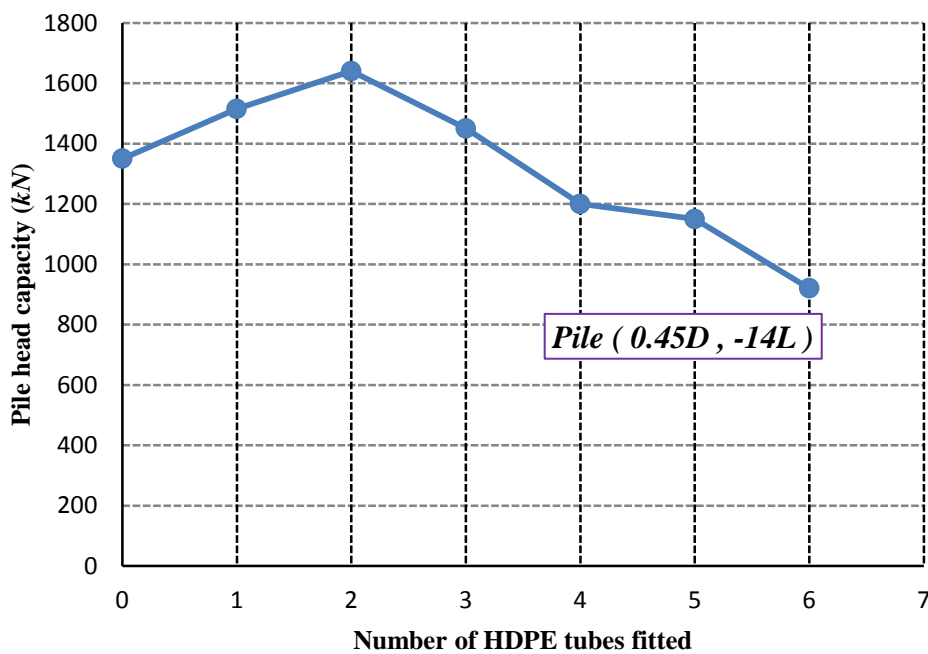
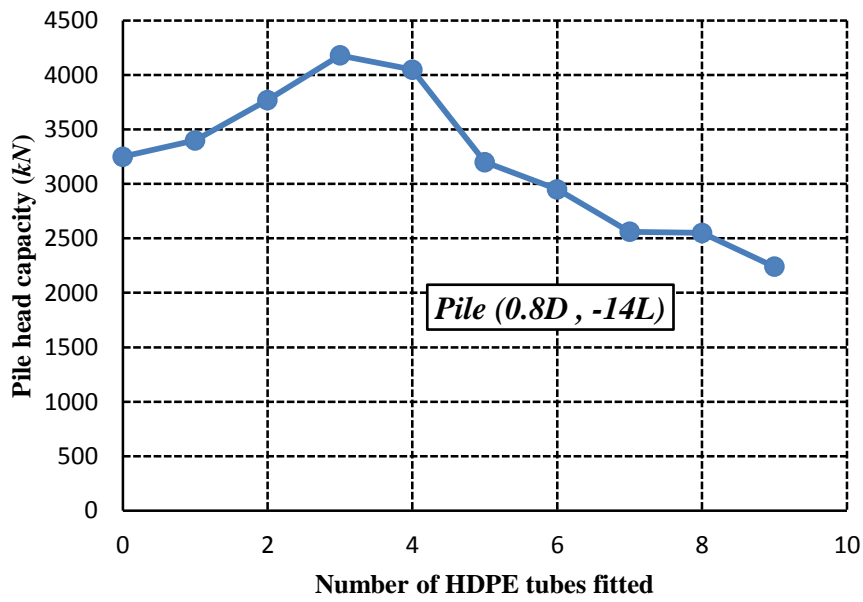
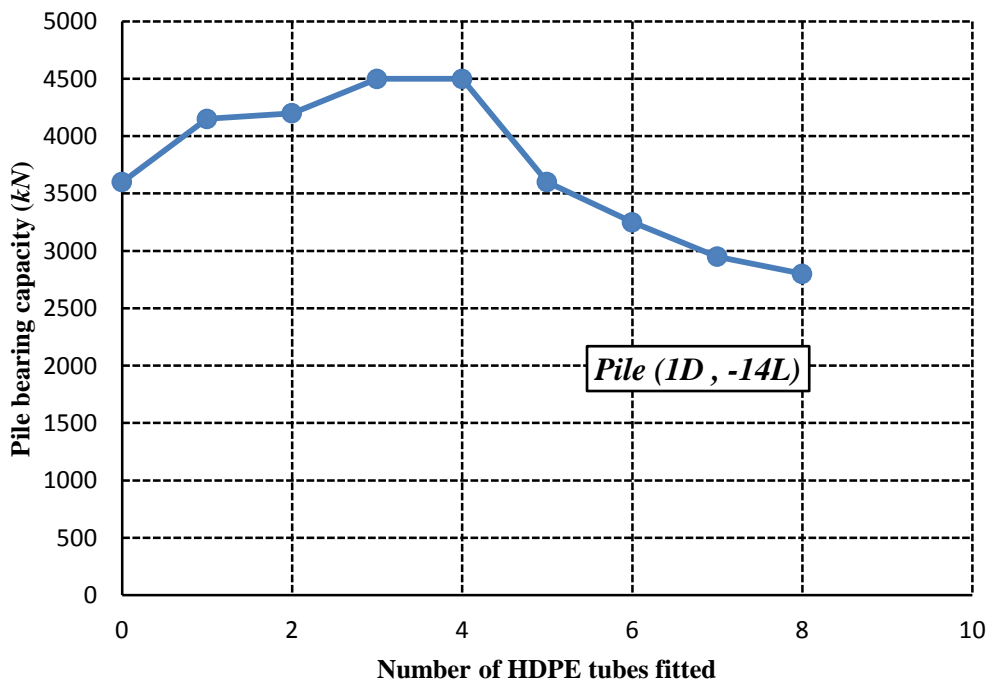


Figure 13: Pile capacity versus number of HDPE tubes for pile (0.45D, -14L).



**Figure 14: Pile capacity versus number of HDPE tubes for pile (0.8D, -14L).**



**Figure 15: Pile capacity versus number of HDPE tubes for pile (1D, -14L).**

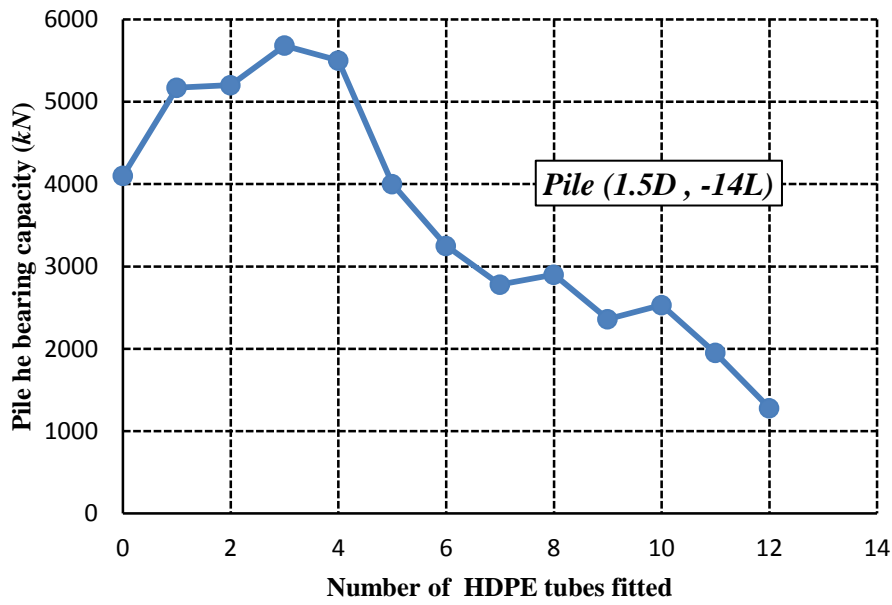


Figure 16: Pile capacity versus number of HDPE tubes for pile (1.5D, -14L)

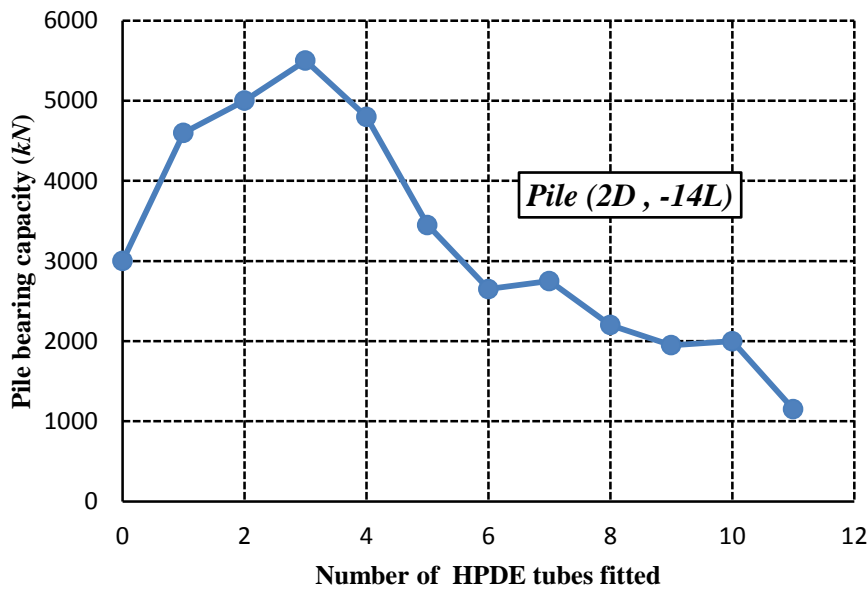


Figure 17: Pile capacity versus number of HDPE tubes for pile (2D, -14L)

## Concluding remarks

At present, despite the increasing use precast concrete piles fitted with energy loops to exploit ground heat, there is very little published guidance to assist engineers in the geotechnical design of such piles. Much of the existing knowledge is proprietary and rests with a select limited number of specialist companies that pioneered the technology behind energy piles. As a result, most engineers are uncertain as to how or even whether energy loops affect the load capacity and settlement behaviour of a piled foundation. Therefore there is a great need for field test data and a reliable method of analysis and design that would be appropriate for energy piles. This is the opportunity identified in the present work to develop a finite element based method which takes into account the unique parameters of energy piles and to assess what effect the presence of the energy loops will have on the bearing capacity and settlement of the piles.

The present research with respect to its objectives demonstrated numerically that the inclusion of HDPE tubes as energy loops extending from the pile base into the bearing soil causes further complex interaction mechanisms and can lead to significant reduction in the bearing capacity of the pile. This negative effect has much to do with degradation of the relative pile-soil stiffness as a result of the additional compressibility created by the tubes if intensely embedded in the bearing soil beneath the pile base. Under the high stresses beneath a pile base cluttered with HDPE tubes, the conventional soil mechanics formulae for ultimate pile base resistance are invalid and there is even a possibility that the mobilisation of shaft resistance in the vicinity of the pile toe is also affected.

Using *PLAXIS 3D* software, numerical analysis of 60 different cases of energy piles showed that, for a typical 2 m diameter pile, fitting 11 HDPE tubes can cause the pile capacity to decrease by as much as 70%. However, with 3-4 HDPE tubes installed, there can be a 30%-75% enhancement of the pile capacity, probably due to optimum reinforcing effect on the soil. There is confidence in these figures, despite not having been corroborated with experimental data, because the computed settlements corresponding to the pile ultimate were always close to 10% of the pile diameter, which is consistent with observed pile behaviour in field tests. In addition, the computed pile capacities for piles without HDPE tubes (conventional pile cases) were found to be consistent with estimates from soil mechanics based formulae. The apparent reliability of the analyses notwithstanding, it is important to validate the results further when full-scale test data from energy piles become available in the future. This is because the complexity of pile-tube-soil systems, which has not been modelled before this research.

## References

Abdelaziz, S. L., Olgun, C. G. and Martin, J. R. (2011). *Design and operational considerations of geothermal energy piles: 08/15/2009-07/31/2010 GeoFrontiers 2011*. Geo-Institute, ASCE, Dallas TX, March 13<sup>th</sup>-16<sup>th</sup>.

Amis, T (2011) *Energy Foundations in the UK* <  
[http://www.gshp.org.uk/GroundSourceLive2011/TonyAmis\\_Piles\\_gsl.pdf](http://www.gshp.org.uk/GroundSourceLive2011/TonyAmis_Piles_gsl.pdf)> [Accessed 30<sup>th</sup> July 2013].

Bouazza, A., Adam, D., Singh, R.M., Ranjith, PG. (2011). *Direct Geothermal Energy from Geostructures*: Australian Geothermal Energy Conference, 16-18 November 2011. Melbourne, p. 245-248.

Bourne-Webb, P. J., Amatya, B., Soga, K., Amis, T., Davidson, C. and Payne, P. (2009). *Energy pile test at Lambeth College, London: geotechnical and thermodynamic aspects of pile response to heat cycles*. *Geotechnique*, Vol. 59, No. 3, p.237-248.

Braja M. D (2006), *Principles of foundation engineering*, 6<sup>th</sup> edn. New York: Wadsworth Publishing Co Inc : distributor Cengage Learning Services: distributor Cengage Learning Australia : distributor Cengage Learning New Zealand : distributor Thomson Learning.

Fleming, K., Weltman, A., Randolph, M., Elson, K (2008). *Piling Engineering*, 3<sup>rd</sup> Edition. New York, NY: Taylor & Francis.

Hamada, Y., Saitoh, H., Nakamura, M., Kubota, H. and Ochifuji, K. (2007). *Field performance of an energy pile system for space heating*. *Energy and Buildings*, Vol. 39, p.517-524. Elsevier.

Happold, B. (2013). *Ground Energy Options*. <  
[http://www.designingbuildings.co.uk/wiki/Ground\\_energy\\_options](http://www.designingbuildings.co.uk/wiki/Ground_energy_options)>. [Accessed 25<sup>th</sup> June 2013].

Khosravi, A., Moradshahi, A., McCartney, J. S., and Kabiri, M. (2016). *Numerical analysis of energy piles under different boundary conditions and thermal loading cycles*. *E3S Web of Conferences*, Vol. 9, No. 05005, E-UNSAT 2016. DOI: 10.1051/e3sconf20160905005.

Laloui, L. and Di Donna, A. (2011) *Understanding the behaviour of energy geo-structures*. *Proceedings of ICE, Civil Engineering*. [Internet]. 164(4), p. 184-191. <  
<http://www.icevirtuallibrary.com/content/article/10.1680/cien.2011.164.4.184>>. [Accessed 19<sup>th</sup>  
April 2013].

Laloui, L., Nuth, M. and Vulliet, L. (2006). *Experimental and numerical investigations of the behaviour of a heat exchanger pile*. *International Journal of Analytical and Numerical Methods in Geomechanics*. Vol. 30, No.8, p763-781.

Ozudogru, T. Y., Olgun, C. G. and Senol, A. (2014). *3D numerical modelling of vertical geothermal heat exchangers*. *Geothermics*, Vol. 51.

Peron, H. and Laloui, L. (2010). *Geotechnical design of heat exchanger piles*. GSHP Association Research Seminar on current and future research into ground source energy. National Energy Centre, Milton Keynes, United Kingdom, January 21<sup>st</sup> 2010.

PLAXIS Ltd. (2006) *Plaxis manual 3D foundation, Version 1.5*. <  
<http://www.civil.iitb.ac.in/~ajuneja/Plaxis%20program/3D%20Foundation%20Introductory/Manuals/English/3DFV15-Reference.pdf>> [Accessed 12<sup>th</sup> July 2013].

Skanska. (2010a) *Modelling of Ground Source Energy*. <  
<http://www.skanska.co.uk/Global/Sevices/Piling/Datasheets/Modelling-of-Ground-Source.pdf> > [Accessed 14<sup>th</sup> March 2013].

Skanska. (2010b) *Energy Piles*. <  
<http://www.skanska.co.uk/Global/Sevices/Piling/Datasheets/Energy-piles.pdf> > [Accessed 14<sup>th</sup> March 2013].

Skanska. (2012) *Energy Piles- Renewable Energy from Foundations*. <  
<http://www.ice.org.uk/getattachment/33f6e360-0301-45f7-b187-f4ba4e4368e1/Energy-Piles---renewable-Energy-from-Foundations.aspx> > [Accessed 14<sup>th</sup> March 2013].

Suryatriyastuti, M.E., Mroueh, H. and Burlon, S. (2012). *Renewable and Sustainable Energy Reviews- Understanding the temperature-induced mechanical behaviour of energy pile foundations*

[Internet]. 16(5), p. 3344-3354. <

<http://www.sciencedirect.com/science/article/pii/S1364032112001566> >. [Accessed 25<sup>th</sup> June 2013].

Wijewickreme, D. (2011) *Advanced Soil Pipe Interaction Research*. [Internet].13(2011), p. 10-11. <

[http://www.civil.ubc.ca/documents/publications/newsletter/2011spring\\_civil@ubc-vol13.pdf](http://www.civil.ubc.ca/documents/publications/newsletter/2011spring_civil@ubc-vol13.pdf) >.

[Accessed 25<sup>th</sup> Sept. 2013].

Pile dia. (m)	Pile length (m)	No. of HDPE tubes
0.45	5	0,1,2,3,4,5,6,7,8
0.45	14	0,1,2,3,4,5,6,6
0.8	14	0,1,2,3,4,5,6,7,8,9
1	14	0,1,2,3,4,5,6,7,8
1.5	14	0,1,2,3,4,5,6,7,8,9,10,11,12
2	14	0,1,2,3,4,5,6,7,8,9,10,11

**Table 1** Assessed 60 pile cases with different L/D ratios and HDPE tubes

Soil layer type	Sand
Drainage type	Drained
$\gamma_{unsat}$	17.6 kN/m <sup>3</sup>
$\gamma_{sat}$	20 kN/m <sup>3</sup>
Dilatancy cut-off	No
$e_{init}$	0.5
$e_{min}$	0
$e_{max}$	999
Rayleigh $\beta$	0
$E$	19x10 <sup>3</sup> kN/m <sup>2</sup>
$\nu$ (nu)	0.3
Consider gap closure	Yes
$G$	7308 kN/m <sup>2</sup>
$E_{oed}$	25.58x10 <sup>3</sup> kN/m <sup>2</sup>
$c_{ref}$	17 kN/m <sup>2</sup>
$\varphi$ (phi)	36°
$\psi$ (psi)	0°
$V_s$	63.79 m/s
$V_p$	119.3 m/s
Set to default values	Yes
$E_{inc}$	0 kN/m <sup>2</sup> /m
$z_{ref}$	0 m
$c_{inc}$	0 kN/m <sup>2</sup> /m
$z_{ref}$	0 m
Tension cut-off	Yes
Tensile strength	0 kN/m <sup>2</sup>
Strength	Rigid
$R_{inter}$	1
$\delta_{inter}$	0
$K_0$ determination	Automatic
$K_{0,x}$	0.4122
$K_{0,y}$	0.4122
$k_x$	0 m/day
$k_y$	0 m/day
$k_z$	0 m/day
$e_{init}$	0.5
$c_k$	1.000 x 10 <sup>15</sup>

Table 2: Material properties for Soil and interfaces (Mohr-Coulomb model)

Identification	Pile	HDPE tubes
$E$	$30 \times 10^6 \text{ kN/m}^2$	$2.3 \times 10^6 \text{ kN/m}^2$
$\gamma$	$24 \text{ kN/m}^3$	$8.5 \text{ kN/m}^3$
<b>Pile type</b>	Predefined	Predefined
<b>Predefined pile type</b>	Massive circular pile	Circular tube
<b>Diameter</b>	$1.5 \text{ m}$	$0.025 \text{ m}$
<b>Thickness</b>	$0 \text{ m}$	$3 \times 10^{-3} \text{ m}$
$A$	$1.767 \text{ m}^2$	$0.2073 \times 10^{-3} \text{ m}^2$
$I_3$	$0.2485 \text{ m}^4$	$0.01278 \times 10^{-6} \text{ m}^4$
$I_2$	$0.2485 \text{ m}^4$	$0.01278 \times 10^{-6} \text{ m}^4$
<b>Rayleigh <math>\alpha</math></b>	0	0
<b>Rayleigh <math>\beta</math></b>	0	0
<b>Skin resistance</b>	Linear	Linear
$T_{top, max}$	$0 \text{ kN/m}$	$0 \text{ kN/m}$
$T_{bot, max}$	$0 \text{ kN/m}$	$0 \text{ kN/m}$
$T_{max}$	$0 \text{ kN/m}$	$0 \text{ kN/m}$
$F_{max}$	$0 \text{ kN}$	$0 \text{ kN}$

**Table 3:** Input material properties for piles and HDPE tubes

<b>Pile case (0.45D , -5L)</b>		
Number of HDPE tubes	Pile Capacity (kN)	Maximum pile head displacement (mm)
0	1890	45.12
1	1690	44.87
2	1680	44.97
3	1420	44.96
4	1400	45.30
5	1400	45.12
6	1150	44.79
7	1120	44.80
8	970	44.85

Table 4: Computed capacities and corresponding settlement for pile (0.45D, -5L).

<b>Pile case (0.45D , -14 L)</b>		
Number of HDPE tubes	Pile Capacity (kN)	Maximum pile head displacement (mm)
0	1350	45.52
1	1515	44.91
2	1640	45.00
3	1450	44.83
4	1200	45.20
5	1150	45.30
6	920	45.16

Table 5: Computed capacities and corresponding settlement for pile (0.45D, -14 L).

<b>Pile case (0.8D , -14L)</b>		
<b>Number of HDPE tubes</b>	<b>Pile Capacity (kN)</b>	<b>Maximum pile head displacement (mm)</b>
0	3250	80.22
1	3400	79.88
2	3770	80.07
3	4180	80.20
4	4050	80.40
5	3200	79.51
6	2950	79.79
7	2560	79.86
8	2550	79.80
9	2240	79.91

Table 6: Computed capacities and corresponding settlement for pile (0.8D, -14L)

<b>Pile case (1D , -14L)</b>		
<b>Number of HDPE tubes</b>	<b>Pile Capacity (kN)</b>	<b>Max. pile head displacement (mm)</b>
0	3600	100.60
1	4150	99.97
2	4200	99.77
3	4500	103.20
4	4500	100.10
5	3600	100.30
6	3250	103.80
7	2950	103.00
8	2800	100.200

Table 7: Computed capacities and corresponding settlement for pile (1D, -14L).

<b>Pile case (1.5D , -14L)</b>		
<b>Number of HDPE tubes</b>	<b>Pile Capacity (kN)</b>	<b>Max. pile head displacement (mm)</b>
0	4100	150.20
1	5170	150.40
2	5200	150.60
3	5680	150.30
4	5500	150.40
5	4000	144.70
6	3250	149.80
7	2780	150.50
8	2900	150.50
9	2630	150.30
10	2530	149.90
11	1950	150.40
12	1280	149.70

Table 8: Computed capacities and corresponding settlement for pile (1.5D, -14L).

<b>Pile case (2D , -14L)</b>		
<b>Number of HDPE tubes</b>	<b>Pile Capacity (kN)</b>	<b>Max. pile head displacement (mm)</b>
0	3000	199.60
1	4600	199.50
2	5000	200.30
3	5500	100.30
4	4800	200.80
5	3450	200.10
6	2650	200.00
7	2750	200.00
8	2200	199.00
9	1950	200.10
10	2000	200.00
11	1150	199.50

Table 9: Computed capacities and corresponding settlement for pile (2D, -14L).